

# Wastewater-boosted biodegradation amplifying seasonal variations of $pCO_2$ in the Mekong–Tonle Sap river system

Ji-Hyung Park • Hyojin Jin · Tae Kyung Yoon · Most Shirina Begum · Eliyan Chea · Eun-Ju Lee · Seung-Cheol Lee · Neung-Hwan Oh

Received: 22 February 2021/Accepted: 15 June 2021/Published online: 29 June 2021 © The Author(s), under exclusive licence to Springer Nature Switzerland AG 2021

**Abstract** Water pollution disrupts the ecological integrity of urbanized river systems, but its impacts on riverine metabolic processes and carbon fluxes are poorly studied in developing countries. Three seasonal field surveys were combined with two high-resolution measurements and an in situ incubation experiment to investigate the effects of untreated wastewater on organic matter biodegradation and the partial pressure of CO<sub>2</sub> (*p*CO<sub>2</sub>) along the Mekong–Tonle Sap network around Phnom Penh. High-resolution measurements

Responsible Editor: Ishi Buffam.

**Supplementary Information** The online version contains supplementary material available at https://doi.org/10.1007/s10533-021-00823-6.

J.-H. Park (⊠) · H. Jin · M. S. Begum Department of Environmental Science and Engineering, Ewha Womans University, Seoul 03760, Republic of Korea e-mail: jhp@ewha.ac.kr

#### T. K. Yoon

Department of Forest Science, Sangji University, Wonju 26339, Republic of Korea

#### E. Chea

Department of Environmental Science, Royal University of Phnom Penh, Phnom Penh, Cambodia

E.-J. Lee · S.-C. Lee · N.-H. Oh Graduate School of Environmental Studies, Seoul National University, Seoul 08826, Republic of Korea during the dry-season survey exhibited large downstream increases in  $pCO_2$  along the Mekong reaches receiving Tonle Sap inflows carrying urban sewage, contrasting with little spatial variation during a monsoon survey when the Mekong floodwater reversed the Tonle Sap flow. The monsoonal and dry-season surveys revealed flooding-induced homogenization and large spatial divergences in dissolved organic carbon (DOC) concentration and its  $\delta^{13}$ C and  $\Delta^{14}$ C between the Tonle Sap and connected Mekong reaches. During the 3-day incubation of Mekong waters, alone or mixed with sewage, a large initial nocturnal increase in pCO<sub>2</sub> in sewage-supplemented river water exceeded the subsequent daytime CO<sub>2</sub> uptake by phytoplankton photosynthesis varying with light exposure. This, combined with the preferential consumption of labile DOC components displaying protein-like fluorescence, implies sewage-enhanced biodegradation of riverine organic matter. These results suggest that neglecting wastewater-enhanced CO<sub>2</sub> production in urbanized river basins during long dry periods can result in a significant underestimation of riverine CO<sub>2</sub> emissions.

**Keywords** Biodegradation · Carbon dioxide · Carbon isotopes · Dissolved organic carbon · Mekong River · Wastewater



## Introduction

Extensive research over recent decades has improved our understanding of the transport and transformation of dissolved organic carbon (DOC), particulate organic carbon (POC), and inorganic carbon in inland waters (Cole et al. 2007; Battin et al. 2009; Raymond et al. 2013; Ward et al. 2017). Despite the increasing recognition of the importance of anthropogenically modified river systems for the global estimates of C exports to the ocean and CO<sub>2</sub> emissions to the atmosphere, an accurate assessment of anthropogenic perturbations to riverine metabolic processes and C fluxes remains elusive (Regnier et al. 2013; Park et al. 2018). Anthropogenic fluxes were estimated to account for up to 40% of all terrestrial export to aquatic systems amounting to 2.5 Pg C yr<sup>-1</sup>, which occur via soil erosion, enhanced weathering, and sewage, contributing 0.8, 0.1, and 0.1 Pg C yr<sup>-1</sup>, respectively (Regnier et al. 2013). While estimating these anthropogenic fluxes is subject to large uncertainties, little is known about the downstream effects of sewage on C fluxes in increasingly urbanized river basins worldwide (Park et al. 2018). In particular, anthropogenically altered C fluxes in large river basins across Asia and Africa demand special attention, because the lack of reliable measurements in these regions represents a primary source of uncertainty in the global estimates of riverine CO<sub>2</sub> emissions (Raymond et al. 2013; Lauerwald et al. 2015).

Although it has long been observed that large loads of sewage containing labile OM can enhance the biodegradation of organic C in urban rivers (Kempe 1984; Frankignoulle et al. 1998; Abril et al. 2002; Griffith and Raymond 2011; Hosen et al. 2014), only a few experimental approaches have addressed the question of how urban sewage alters organic C mineralization in downstream rivers (Begum et al. 2019; Kim et al. 2019). The information gap is particularly daunting regarding organic C dynamics and CO<sub>2</sub> outgassing in rivers draining large population centers across developing countries (Park et al. 2018). Given that 4.1 billion people lack access to improved sanitation, including sewage treatment in 2010 (Baum et al. 2013), untreated wastewater may continue to increase its proportion in the global riverine C transport, stimulating organic matter (OM) biodegradation via synergistic interactions among organic moieties of different lability (Hosen et al. 2014; Begum et al. 2019). Although many experimental studies have recently tested the so-called "priming effects" hypothesis in which the biodegradation of less reactive or recalcitrant riverine OM can be stimulated by the interaction with highly reactive materials such as algal exudates (Bianchi 2011; Bengtsson et al. 2018; Ward et al. 2019), it remains largely unknown whether wastewater can have "non-additive effects" on the biodegradation in large rivers (Bengtsson et al. 2018) and how treated and untreated wastewater would differ in these priming effects (Kim et al. 2019).

Rapid urbanization around several local population centers in the Lower Mekong Basin, together with recent explosions in dam construction along the upper basin in China and many lower basin tributaries, poses unprecedented threats to the ecological integrity and services of aquatic ecosystems (Sabo et al. 2017). Seasonal field surveys were combined with cruise underway measurements and an in situ incubation experiment under different light conditions to examine the effect of untreated wastewater on OM biodegradation and CO<sub>2</sub> production along the Mekong-Tonle Sap network around Phnom Penh, Cambodia. Specifically, we tested the hypothesis that during the dry season, the Tonle Sap inflow carrying untreated wastewater can boost OM biodegradation in the downstream Mekong reaches to such a degree that CO<sub>2</sub> production resulting from enhanced biodegradation may outweigh the phytoplankton CO2 uptake. During two field surveys, we conducted high-frequency underway measurements of the partial pressure of  $CO_2$  ( $pCO_2$ ) along the connected reaches of the two rivers under two contrasting flow conditions to compare the spatial variations in  $pCO_2$  between the monsoon and dry periods. To explain the large spatial variability in CO<sub>2</sub> concentrations during the dry season, an in situ incubation experiment was performed with river water, alone or mixed with sewage, under natural light versus dark conditions. This approach combining high-resolution field measurements of pCO<sub>2</sub> and in situ incubation experiments was expected to provide empirical evidence of localized intense effects of urbanization on riverine metabolic processes and C fluxes.



## Methods

Study site

The Mekong River originates in the eastern Tibetan Plateau and runs 4763 km through China, Myanmar, Lao PDR, Thailand, Cambodia, and Vietnam into the South China Sea, with a mean annual discharge of 446 km<sup>3</sup> (Mekong River Commission 2019). This study was conducted in the Cambodian part of the Lower Mekong River Basin around the Tonle Sap River confluence (Fig. 1). The 120 km long Tonle Sap has a unique natural flow regime during the flood period from June to October: the floodwater from the Mekong upstream of Phnom Penh during the monsoon season reverses the Tonle Sap flow and also flows overland across the large floodplains into the Tonle Sap Lake, expanding the lake surface area from about 2500 km<sup>2</sup> during the peak dry period up to 17,500 km<sup>2</sup> (Campbell et al. 2009). When the Mekong inflow decreases in November, the Tonle Sap flows back from the lake to the Mekong. The annual precipitation in the Mekong subbasin belonging to the Cambodian territory is 1741 mm, with the bulk (1607 mm) falling during the months from April to October and relatively small dryseason rainfalls (134 mm) from November to March (Mekong River Commission 2019).

The seasonally inundated forests and wetlands in the Tonle Sap Basin provide large sources of OM and nutrients to the connected Mekong-Tonle Sap system. The rapidly growing urban population in Phnom Penh (> 2.2 million in 2019) discharges an ever-increasing load of untreated sewage into sewage drains that are channeled to wetlands or lakes used as sewage retention ponds (Global Green Growth Institute 2019). Urban drainage flowing north is retained in the Lake Boeng Pung Peay before being discharged to the Tonle Sap, while about 80% of sewage flows south and is retained in a network of wetlands and lakes (e.g., Boeung Tumpun and Boeung Choeung Ek) before being discharged to the Tonle Sap or the Bassac River (here considered as the left branch of the Mekong downstream of the Tonle Sap confluence; Fig. 1).

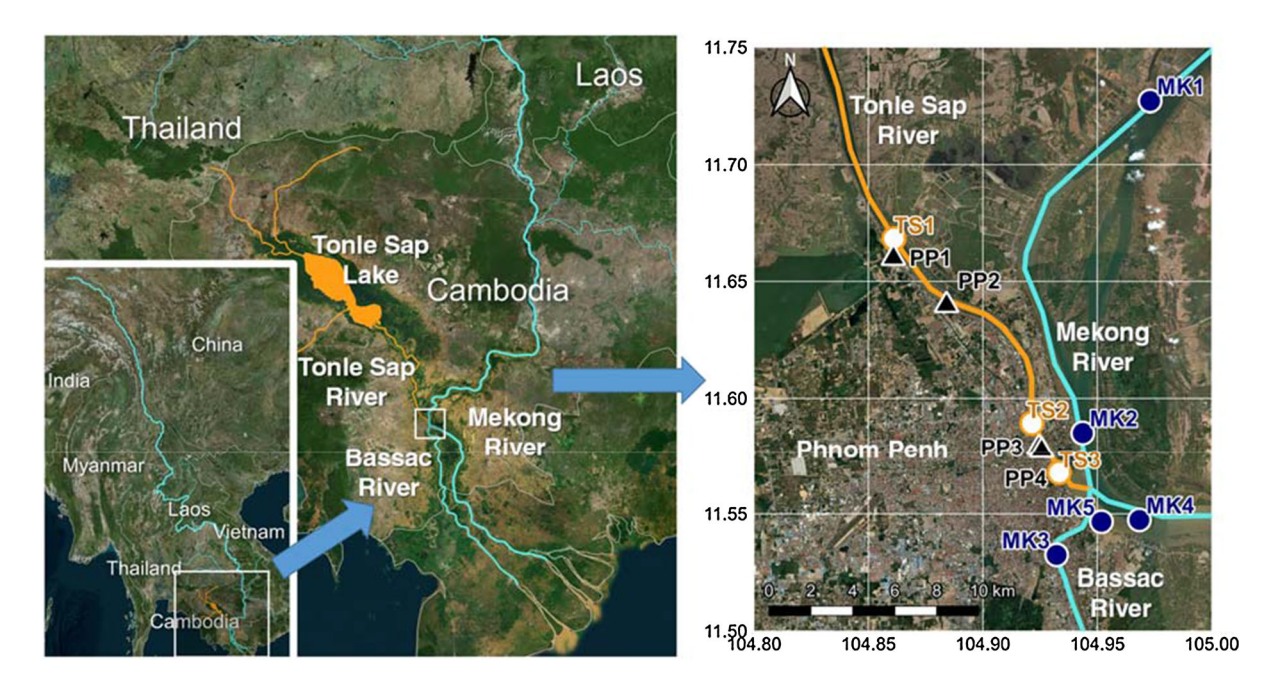


**Fig. 1** The study map showing the sampling sites in the Lower Mekong Basin near Phnom Penh, Cambodia. The inset map shows the location of the sampling sites in the Mekong Basin. Sampling sites include four urban streams or wastewater drains

(PP1-PP4), the Mekong River (MK1-MK4), and the Tonle Sap River derived from the Tonle Sap Lake (TS1-TS3). An in situ incubation experiment was conducted at MK5. (Color figure online)



Seasonal field surveys and high-frequency underway *p*CO<sub>2</sub> measurements

We performed a dry-season field survey in January 2017 (January 13-16) and two monsoon surveys in July 2014 (July 8–14) and August 2017 (August 31– September 1). During each field survey, in situ water quality measurements and sampling were conducted at 11 sites within the Mekong-Tonle Sap system around Phnom Penh (Fig. 1), including four mainstem Mekong sites (MK 1, 2, 3, and 4; MK4 was not sampled in July 2014), three Tonle Sap sites (TS 1, 2, and 3), and four sewage sites (PP 1, 2, 3, and 4; PP3 and PP4 could not be sampled in August 2017 because of flooding). While PP1 (Prek Pnov) and PP2 (Svay Pak) are highly polluted streams draining sewage retention ponds, PP3 and PP4 are constructed sewage drains that discharge sewage collected in an urban center of Phnom Penh to the lower reach of the Tonle Sap (Fig. 1). Discrete measurements of water temperature, pH, electrical conductivity, and dissolved oxygen (DO) were conducted in situ with a field multi-meter (Orion 5-Star Portable, Thermo Scientific, USA), while air temperature and barometric pressure were measured by a portable sensor (Watchdog 1650 Micro Station, Spectrum Technologies, USA). Water samples were collected at one point 10–20 cm below the water surface in the middle of the river channel or from the bank of sewage drains. Acid-washed polycarbonate bottles were filled with water to capacity to minimize headspace. Since these discrete samples had to be collected for short sampling times during or between the cruise underway measurements, replicate samplings covering cross-channel variation were not possible.

During the two surveys in 2017, a manual head-space equilibration method (for spot measurements), along with a membrane-enclosed CO<sub>2</sub> sensor system and an equilibrator system for cruise underway measurements in the case of the January survey, was used to measure the surface water concentrations of CO<sub>2</sub> following the protocols established from rigorous laboratory and field tests (Yoon et al. 2016). The membrane-enclosed sensor system consisted of a CO<sub>2</sub> sensor (GMT222, Vaisala, Finland) wrapped in water-impermeable polytetrafluoroethylene (PTFE) membrane tubing (200-07, International Polymer Engineering, USA) and a data logger (CR1000, Campbell Scientific Inc., USA), as has been described in detail

by Yoon et al. (2016). Only the membrane-enclosed CO<sub>2</sub> sensor system was employed for both spot and cruise underway measurements during the first survey in 2014. For headspace equilibration, a 60 mL polypropylene syringe was used to collect a 30 mL water sample from 10 to 20 cm below the water surface, talking care to avoid air bubbles in the syringe. The syringe was then filled with a 30 mL ambient air sample collected at 1 m above the water surface. After vigorously shaking the syringe for 2 min, some of the equilibrated air ( $\sim$  20 mL) was transferred to a pre-evacuated 12 mL glass vial (Exetainer, Labco, UK) to create overpressure in the storage vial; prior tests confirmed no concentration change in the evacuated vials over 6 months. The surface water concentration of CO<sub>2</sub> was calculated from the gas concentrations in the equilibrated air and ambient air samples, barometric pressure, and water temperature based on Henry's law (Hudson 2004). According to Henry's law, the mole fraction of the dissolved gas (xg) at equilibrium can be determined from the partial pressure of the gas  $(p_g)$  and the Henry's law constant (H), following the equation:  $x_g =$ p<sub>o</sub>/H. The total gas concentration (TC) in the original water sample was calculated from the aqueous gas concentration which partitioned into the gas phase at equilibrium (C<sub>AH</sub>) and the aqueous phase concentration which remained in the aqueous phase at equilibrium ( $C_A$ ):  $TC = C_{AH} + C_A$ . The calculated surface water concentration was expressed in either dissolved  $CO_2$  (mg C L<sup>-1</sup>) or  $pCO_2$  (µatm), the latter of which was calculated by reapplying the Henry's law equation.

In July 2014 and January 2017, cruise underway measurements of pCO<sub>2</sub> were taken at intervals of 60 s (July 2014) or 10 s (January 2017) along the Mekong-Tonle Sap near the confluence of the two rivers to examine seasonal differences in the effects of urban wastewater discharged from the Phnom Penh metropolitan area on the  $pCO_2$  levels along the downstream river reaches (Fig. 1). A membraneenclosed CO<sub>2</sub> sensor, alone in July 2014 or combined with a spray-type equilibrator connected to an infrared gas analyzer (IRGA; LI820, Li-Cor, USA) (Yoon et al., 2016) in January 2017, was immersed  $\sim 20$  cm from the surface (July 2014) or in an onboard container (January 2017), which was continuously filled with river water drawn from a depth of 20 cm below the water surface at a rate of 3.5 L min<sup>-1</sup> using



a bilge pump (Tsunami T800, Attwood Co., USA). Along with  $pCO_2$ , basic water quality parameters were measured using a portable multiparameter meter (6820 V2, YSI Inc., USA). To avoid excessive turbulence caused by the boat, the boat speed was maintained at < 10 km h<sup>-1</sup> based on prior tests (Yoon et al. 2017). At the four Mekong and three Tonle Sap sites, manual headspace equilibration was performed onboard during a short mooring (< 30 min) to check sensor measurement accuracy. The air temperature and barometric pressure were recorded in a micrologger (Watchdog 1650 Micro Station, Spectrum Technologies Inc., USA). The cruises were tracked using a GPS tracking unit (Montana 650, Garmin Ltd., USA).

As the two high-frequency measurement systems and the manual equilibration method produced comparable results for the separately collected water samples within < 5% error ranges, we report only the equilibrator data for the ongoing measurements in January 2017. The headspace air in the equilibrator chamber was circulated through a channel connecting the chamber, an air filter, a desiccant (Drierite) column, and an IRGA. The actual water-saturated  $pCO_2$  in the equilibrator was calculated from the  $pCO_2$ measured in dry air entering the analyzer, barometric pressure, water temperature, and equilibrium water vapor (Crawford et al. 2016). The  $pCO_2$  in the equilibrator was then corrected to the water temperature using a temperature effect coefficient. The time lags of the measured  $pCO_2$  resulting from the residence time in the water circuit and the response time of the sensors were corrected using an equation consisting of the hydraulic-corrected sensor output, water circuit residence time, sensor response time, and instantaneous rate of sensor output change (Crawford et al. 2016). Diel variations in  $pCO_2$  may have been a minor factor affecting pCO2 levels in turbid waters during monsoon surveys. The dry-season cruise measurements in January 2017 were conducted for 3 h in the morning, so diel variations during the short measurement period might have been negligible, as confirmed by 3-day high-frequency measurements performed as part of an in situ incubation experiment at site MK5.

# In situ incubation experiment

In conjunction with the field survey in January 2017, an in situ incubation experiment was conducted for 3 days at site MK5, 3 km downstream of the Tonle Sap confluence (Fig. 1). River samples from upstream (MK2) and downstream (MK4) locations were incubated in closed containers that were immersed below the water surface, using the buoys moored  $\sim 2$  m off a pier. To simulate the effect of tributary mixing, two MK2 samples were mixed with a sewage sample collected at PP3 at a ratio of 9:1. All samples were incubated in situ under two light conditions: "alldark" (containers covered with aluminum foil) and natural (alternating dark-light) conditions (transparent polycarbonate or glass containers exposed to natural light). Along with the incubation samples, we also measured  $pCO_2$  at a depth of 20 cm below the water surface by deploying a membrane-enclosed CO<sub>2</sub> sensor connected to the mooring buoys. All sensor measurements of CO<sub>2</sub>, air and water temperature, barometric pressure, and light intensity were logged at 10-s intervals using a data logger (CR1000, Campbell Scientific Inc., USA).

Both "Mekong-only" treatments consisted of three closed polycarbonate bottles (250 mL) filled with 125 mL water sample and a 1200 mL polycarbonate bottle that was filled with 600 mL of water and then installed with a membrane-enclosed CO<sub>2</sub> sensor to measure headspace *p*CO<sub>2</sub>. Both mixture treatments were performed in only one 1200 mL polycarbonate bottle installed with a CO<sub>2</sub> sensor. Therefore, chemical analyses were performed with the single 600 mL water samples of the mixture treatments and the three replicate samples (125 mL each) and one 600 mL sample of the Mekong-only treatments.

## Chemical analyses

Headspace and ambient air samples collected in preevacuated vials were injected into a gas chromatograph (GC; 7890A, Agilent, USA) equipped with a Supelco Hayesep Q 12 ft 1/8" column for CO<sub>2</sub> measurement. More detailed instrumental settings have been reported elsewhere (Jin et al. 2018). Standard reference gases in the N<sub>2</sub> balance were used to calibrate the GC signals. Headspace equilibration samples collected during the surveys in January 2017 and August 2018 were analyzed for stable C isotope



ratios in  $CO_2$  ( $\delta^{13}C_{CO2}$ ) using a GasBench-IRMS (ThermoScientific, Bremen, Germany) at the UC Davis Stable Isotope Facility.

Water samples were transported on ice to a laboratory at the Royal University of Phnom Penh within a few hours of collection. In 2014 and August 2017 samples were immediately filtered through a precombusted glass fiber filter (GF/F, Whatman; nominal pore size 0.7 µm) and frozen. In January 2017 samples were immediately frozen and then shipped to Ewha Womans University where thawed samples were filtered before analyzing DOC and optical properties within a week after the sampling. As part of the quality control of all chemical analyses, a standard with a known concentration was analyzed for every batch of ten samples. In addition, duplicate samples were analyzed for approximately 10% of all analyzed samples to check the instrumental stability and precision. Total suspended solids (TSS) were measured as the difference in the weight of the dried (60 °C for 48 h) filter before and after filtering the water sample. Filtered water samples were analyzed for DOC concentration on a total organic carbon (TOC) analyzer (TOC-V<sub>CPH</sub>, Shimadzu, Japan), which employs thermal detection of CO<sub>2</sub> from hightemperature OM combustion. The concentrations and  $\delta^{13}$ C of POC collected on the GF/F filters were measured using an IRMS (ThermoScientific, Bremen, Germany) at the Physical Research Laboratory, Ahmedabad, India.

The UV absorbance of the filtered water samples was measured across the wavelength range of 200 to 1100 nm using a UV-Vis spectrophotometer (8453, Agilent, USA). Fluorescence excitation-emission matrices (EEMs) were measured on a fluorescence spectrophotometer (F7000, Hitachi, Japan) by simultaneous scanning over excitation wavelengths from 200 to 400 nm at 5 nm intervals and emission wavelengths from 290 to 540 nm at 1 nm intervals. Major fluorescent DOM components were identified using parallel factor analysis (PARAFAC; Stedmon and Bro 2008) in MATLAB with EEMs measured for 47 samples from the Lower Mekong River, following the methods described in detail by Begum et al. (2019). Three identified components were termed C1 (peak excitation/emission wavelengths: 350/450 nm), C2 (275/345 nm), and C3 (310/405 nm), which correspond to "humic-like", "protein-like", and "microbial humic-like" fluorescence, respectively, as

reported in previous studies (Fellman et al. 2010). Although the highly bioavailable protein-like peak has usually been associated with aromatic amino acids derived from microbial biomass, the molecular-level analysis of this fluorescent organic fraction has suggested that low molecular weight aromatics of plant origin can also contribute to the same fluorescence peak (Stubbins et al. 2014). Absorbance and fluorescence data were also processed to calculate the specific UV absorbance at 254 nm (SUVA<sub>254</sub>) (Weishaar et al. 2003), fluorescence index (FI) (McKnight et al. 2001), and humification index (HI) (Zsolnay et al. 1999).

Dual carbon isotope analyses of dissolved inorganic carbon (DIC) were conducted with water samples from the field survey in July 2014, which had been supplemented with saturated HgCl<sub>2</sub> immediately after sampling to minimize microbial activity. The water sample was acidified using 40% H<sub>3</sub>PO<sub>4</sub> solution to convert DIC to CO2, which was then separated cryogenically using a liquid N<sub>2</sub> trap in a vacuum line and sealed in a pre-combusted Pyrex tube. Dual carbon isotope analyses of DOC were conducted with the frozen filtered water samples from field surveys in July 2014 and January 2017. Each water sample was acidified using a 40% H<sub>3</sub>PO<sub>4</sub> solution to remove inorganic carbon in the form of CO<sub>2</sub>. After sparging the acidified sample with helium gas, the sample was irradiated with UV in a quartz reactor for 4 h to oxidize it with ultrahigh purity O<sub>2</sub> (Raymond and Bauer 2001). The produced CO<sub>2</sub> in the oxidation step was cryogenically separated using a liquid N<sub>2</sub> trap in a vacuum line and sealed in a precombusted Pyrex tube. The separated, sealed CO<sub>2</sub> samples generated from DIC and DOC were sent to the National Ocean Sciences Accelerator Mass Spectrometry (NOSAMS) facility at the Woods Hole Oceanographic Institution for dual carbon isotope analysis  $(\Delta^{14}C \text{ and } \delta^{13}C)$ . The CO<sub>2</sub> samples were reduced to graphite targets for  $\Delta^{14}$ C analysis at NOSAMS. Accelerated mass spectrometry and isotope ratio mass spectrometry were used for  $\Delta^{14}C$  and  $\delta^{13}C$  analyses, respectively (http://www.whoi.edu/nosams/home).



## Results

Seasonal field surveys and high-frequency underway measurements

When in situ water quality measurements (Table S1) and carbon concentrations (Table 1) measured during the dry-season survey in January 2017 were compared with the corresponding data from the two monsoon surveys in July 2014 and August 2017, the sewage drain sites did not exhibit any clear seasonal differences. However, the dry-season measurements in January 2017 displayed pronounced longitudinal changes along the Mekong-Tonle Sap, in contrast to the homogenized spatial patterns observed during the two monsoon surveys. For example, monsoonal concentrations of DOC in the two rivers ranged from 1.7 to  $2.3 \text{ mg C L}^{-1}$ , whereas in January 2017 the relatively low DOC concentration at MK2 (1.3 mg C  $L^{-1}$ ) increased up to 3.0–3.6 mg C  $L^{-1}$  at MK3 and MK4 in response to the high-DOC inflow from the Tonle Sap  $(3.5 \text{ mg C L}^{-1})$ . The distinct longitudinal variations in DOC concentrations observed during the January 2017 survey were also reflected in the corresponding variations in the intensity of fluorescent peaks identified in fluorescence EEMs (Fig. S1). Despite the limitation of a small number of samples, similar longitudinal variations in the concentrations and  $\delta^{13}$ C values of POC and CO<sub>2</sub> along the Mekong indicated a noticeable tributary influence during the dry season (Table 1).

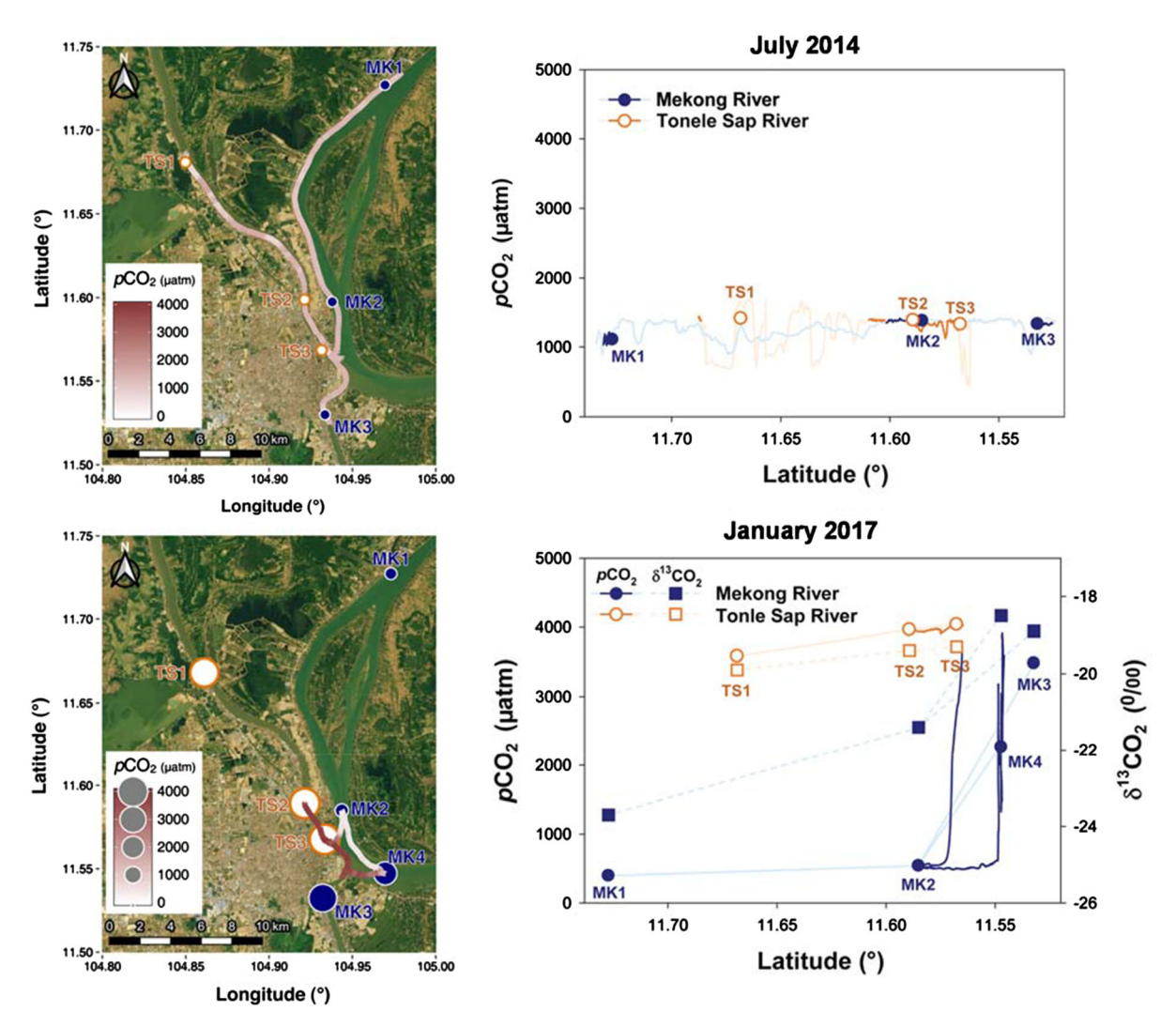
The transects of pCO<sub>2</sub> from the high-frequency underway measurements in January 2017 showed large increases in  $pCO_2$  and  $\delta^{13}C-CO_2$  along the Mekong reaches downstream of the Tonle Sap confluence. This is in sharp contrast to the July 2014 transects of pCO<sub>2</sub> that displayed relatively small spatial variations, except for the sections where the boat moved faster than the predetermined speed, resulting in large fluctuations in  $pCO_2$  (Fig. 2). Despite the overall homogenizing effect of the Mekong floods on the  $pCO_2$  levels in the Tonle Sap, slightly higher levels of  $pCO_2$  were found along the upper reach of the Tonle Sap than in the lower reach near the confluence in July 2014, which was consistent with the higher  $pCO_2$  found at TS1 than at the lower TS sites during the second monsoon survey in August 2017 (Table 1). A large dry-season increase was observed from 381 µatm (MK1) to 3119 µatm (MK3) along the Mekong in January 2017, illustrating a significant contribution of the Tonle Sap to the Mekong's longitudinal transition from autotrophy to

Table 1 Summary of carbon chemistry measured along the Mekong-Tonle Sap river system around Phnom Penh, Cambodia

River	Site	DOC (	mg C L	1)	POC (n	ng C L <sup>-1</sup> )	δ <sup>13</sup> C-P0	OC (‰)	<i>p</i> CO <sub>2</sub> (μ	atm)		δ <sup>13</sup> C-CO <sub>2</sub> (‰)	
		Jul-14	Jan-17	Aug-17	Jan-17	Aug-17	Jan-17	Aug-17	Jul-14	Jan-17	Aug-17	Jan-17	Aug-17
Mekong	MK1	2.1	1.0	1.7	0.6	1.9	- 26.4	- 28.3	1107	433	2016	- 23.7	- 21.3
	MK2	2.0	1.3	1.7					1381	606	1987	- 21.4	- 19.3
	MK3	2.1	3.6	1.8	0.8		- 30.1		1333	3506	1846	- 18.9	- 19.3
	MK4		3.0	2.0	0.8	1.6	- 30.8	- 27.4		2016	1911	- 18.5	- 19.2
Tonle Sap	TS1	2.0	4.4	2.3					1413	3768	4140	- 19.9	- 18.5
	TS2	2.0	4.2	1.8					1388	3740	1860	- 19.4	- 21.4
	TS3	2.0	3.5	1.7	1.0	1.1	- 30.7	- 27.7	1328	3928	1863	- 19.3	- 19.2
Sewage	PP1	16.5	7.2	8.9					> 5000	1766	1101	- 19.3	- 13.5
	PP2	6.3	10.1	10.5	5.8	4.7	- 25.6	- 26.6	> 5000	34,151	27,349	- 15.2	- 12.2
	PP3	48.2	50.2		36.7		- 25.2		> 5000	20,984		- 18.6	
	PP4	8.5	5.6						> 5000	17,606		- 22.8	

Field surveys were conducted at three (only in July 2014) or four Mekong (MK) and three Tonle Sap (TS) locations as well as two (only in July 2017) or four sewage drains during a dry season (January 2017) and two monsoon seasons (July 2014 and August 2017). While  $pCO_2$  was measured in July 2014 using  $CO_2$  sensors with the upper detection limit around 5000  $\mu$ atm, the data for the other seasons were obtained using the manual headspace equilibration method. POC and  $\delta^{13}$ C-POC were measured only for the presented sites. Part of the data collected in 2017 were reported in a regional comparison study by Begum et al. (2021)





**Fig. 2** Sampling locations and two high-frequency underway measurements of  $pCO_2$  along the Mekong–Tonle Sap river near Phnom Penh, Cambodia. While the monsoon  $pCO_2$  data (July 2014; upper right panel) were obtained using a membrane enclosed sensor, the dry-season data (January 2017; lower right panel) were collected using an equilibrator system,

complemented with a manual headspace equilibration method (circles) and the analysis of  $\delta^{13}\text{C-CO}_2$  (squares). Note that the  $p\text{CO}_2$  data in July 2014 are distinguished by the measurements obtained at the predetermined boat speed (bolder lines) and those at the faster boat speeds (thin lines). (Color figure online)

heterotrophy along the short stretch around the confluence. Given the relatively large  $p\text{CO}_2$  level at the most upstream Tonle Sap location from the Phnom Penh metropolitan area (TS1; Table 1), the increased proportion of the  $\text{CO}_2$ -rich Tonle Sap flow in the downstream reach of the Mekong during the dry season can explain the observed tributary effect on the Mekong  $p\text{CO}_2$ . A further downstream increase in  $p\text{CO}_2$  along the Tonle Sap (3341 to 3472  $\mu$ atm), combined with exceptionally large  $p\text{CO}_2$  values at the

four sewage drain sites (Table 1), indicated a strong sewage influence on the  $pCO_2$  levels of both the Tonle Sap and the downstream reaches of the Mekong.

As with DOC and  $CO_2$  concentrations,  $\delta^{13}C$  and  $\Delta^{14}C$  values of DOC and DIC measured in July 2014 were clustered within a narrow range, whereas the values measured in January 2017 exhibited unique longitudinal variations, indicating a shift of the Mekong DOM toward the Tonle Sap isotopic signatures (Fig. 3). While the tightly clustered values of



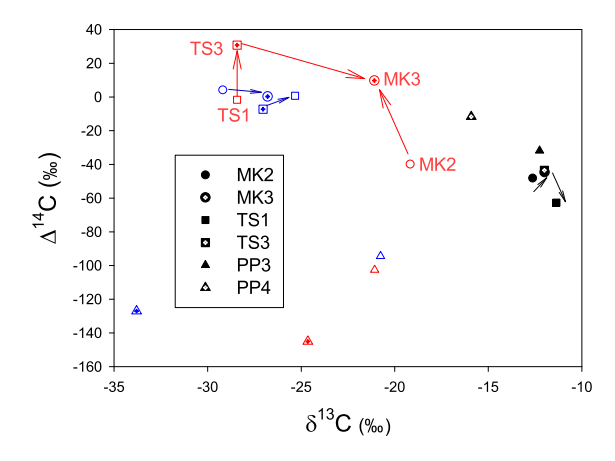


**Fig. 3** Spatial variations in  $\delta^{13}$ C and  $\Delta^{14}$ C of DOC and DIC across the Mekong–Tonle Sap river system around Phnom Penh, Cambodia. While the same symbols are used for the same sites in the Tonle Sap, Mekong, and urban sewage drains (PP), different colors indicate either different times or parameters (black: DIC in July 2014; blue: DOC in July 2014, red: DOC in January 2017). Arrows indicate the prevailing flows along the Mekong-Tonle Sap. (Color figure online)

 $\delta^{13}C$  and  $\Delta^{14}C$  indicated the homogenizing effect of the Mekong-driven reversed flow of the Tonle Sap on the monsoonal C dynamics in the connected rivers, the increased proportion of the Tonle Sap inflow in the downstream Mekong flow in January 2017 resulted in a distinct increase in  $\Delta^{14}C$ -DOC but a slight decrease in  $\delta^{13}C$ -DOC along the Mekong reach from MK2 to MK3. However, distinctively lower  $\Delta^{14}C$  values at the two sewage drain sites (– 94.4‰ to –145.1‰) indicated older ages of the sewage-derived DOM than those of the two rivers (– 39.8‰ to 30.8‰).

## In situ incubation experiment

During the 3-day incubation, the concentrations of DOC and CO<sub>2</sub> changed only slightly in the upstream Mekong samples (MK2), whereas distinct initial increases in CO<sub>2</sub> were found in the MK4 and mixture samples (Table 2; Fig. 4). DOC concentrations in the Mekong-only samples slightly increased (MK2) or little changed (MK4) under both natural light and all-dark conditions, indicating a net production of DOC from the particles including microbial biomass. In contrast, the DOC concentrations in the mixtures of Mekong water (MK2) and sewage (PP3) decreased by 24 and 3% under all-dark and natural light conditions, respectively. The mixture samples exhibited a pronounced large initial nocturnal increase in the

concentration of  $CO_2$  (1.2–1.3 mg C  $L^{-1}$ ), which amounted to 35–38% of the initial DOC concentration of each sample, and far exceeded the subsequent day-time  $CO_2$  uptake equivalent to 0.5 and 0.1 mg C  $L^{-1}$  for the all-dark and natural light treatments, respectively.

In the MK2 samples incubated under natural light conditions, the daytime  $CO_2$  uptake exceeded the nocturnal  $CO_2$  production for the first 2 days, resulting in an overall  $CO_2$  sink of 0.3 mg C L<sup>-1</sup>. Compared to the small initial  $CO_2$  changes in the MK2 samples, the increases in the MK4 samples (0.29–0.34 mg C L<sup>-1</sup>) were appreciable during the first night (Table 2), indicating the strong influence of the Tonle Sap inflow on DOC concentration and lability in the short stretch around the confluence. However, the greater nocturnal  $CO_2$  production in the MK4 samples relative to the initial day-time uptake of  $CO_2$  was reversed in the following two days, resulting in an overall  $CO_2$  sink (0.4 mg C L<sup>-1</sup>) exceeding that of the upstream MK2.

Differential EEMs obtained by subtracting the fluorescence intensities of the pre-incubation samples from those of the post-incubation samples provided a visual representation of potential sources and transformations of major DOM components (Fig. 5). Under all-dark conditions, the Mekong samples from MK2 and MK4 displayed distinct decreases in fluorescence intensities across the EEM region indicative of protein-like fluorescence (C2 component in Fig. S2; Fellman et al. 2010). The decrease in protein-like fluorescence was more pronounced in the MK4 samples than in the MK2 samples. When the differential EEMs of the MK4 samples were compared with those of the mixture samples, the predominant changes in the differential EEM of the MK4 samples incubated in the dark were found across the same EEM region as those of the mixture samples around the protein-like peaks (Fig. 5), implying a preferential consumption of labile organic materials in the downstream Mekong. In contrast, both Mekong-only samples (MK2 and MK4) incubated under natural light conditions exhibited decreases in humic-like fluorescence peaks (C1 in Fig. S2), but increases in peak areas encompassing protein-like and microbial humic-like components (C3 in Fig. S2), with more pronounced changes in fluorescence intensity in the MK4 sample than in the MK2 sample.



Table 2 Short-term changes in DOC and CO2 concentrations during an in-situ incubation in the Lower Mekong River for 3 days in January 2017

Sample	Incubation	$DOC \; (mg \; C \; L^{-1})$	g C L <sup>-1</sup> )	BDOC		CO <sub>2</sub> ch	CO <sub>2</sub> change (mg C L <sup>-1</sup> )	$C L^{-1}$						
		Initial	Final	$(mg C L^{-1})$	(%)	1st		2nd		3rd		Sum		
						Night	Day	Night	Day	Night	Day	Night	Day	Whole
	Duration (h)					10.8	11.7	12.3	11.7	12.3	4.7	35.4	28.1	63.5
Mekong-Up (MK2)	Dark	1.3	1.5	- 0.3	- 21.8	0.07	0.02	0.02	0.02	0.03	0.00	0.11	0.05	0.17
			(0.1)											
	Light	1.3	1.5	- 0.2	- 16.6	0.07	-0.23	0.02	-0.17	0.02	- 0.01	0.12	- 0.41	- 0.29
			(0.1)											
Mekong-Down (MK4)	Dark	2.9	2.8	0.0	8.0	0.29	90.0	0.07	0.02	0.09	- 0.08	0.45	0.00	0.45
			(0.1)											
	Light	2.9	3.0	- 0.1	- 3.2	0.34	- 0.21	0.05	- 0.55	0.03	- 0.05	0.42	- 0.81	-0.39
			(0.1)											
Mixture $(9:1)$ (MK2 + PP3) Dark	Dark	3.4	2.6	8.0	23.7	1.21	0.52	0.92	0.50	0.22	90.0	2.36	1.08	3.44
	Light	3.4	3.3	0.1	2.9	1.31	0.09	0.95	- 1.49	0.71	- 1.04	2.97	- 2.43	0.54

Incubation bottles containing unfiltered Mekong waters (MK2 and MK4), alone or mixed with a sewage (PP3), were immersed in the surface water under the natural light ("dark") conditions. The final DOC concentrations of the Mekong-only samples and mixture samples are presented by the means of four replicate (followed by one standard error in parentheses) and single measurements, respectively. Biodegradable DOC (BDOC) was calculated as the difference in the initial and mean final concentrations of DOC



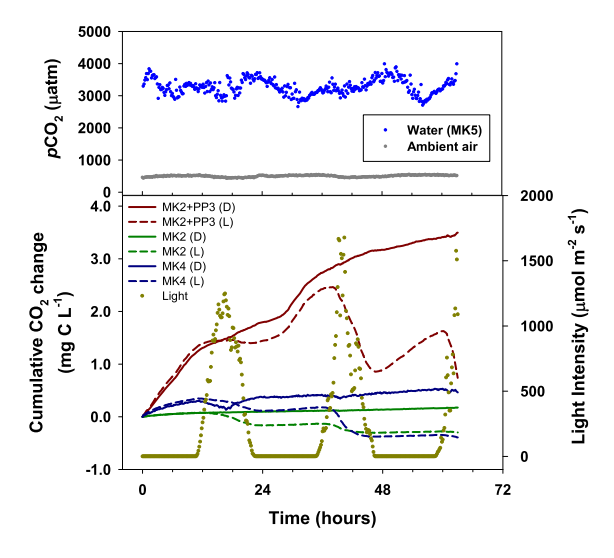


Fig. 4 High-frequency measurements of in-stream  $pCO_2$  and cumulative  $CO_2$  changes in the headspace of the bottles of three types of waters incubated at site MK5 under all-dark (D) or natural light (L) conditions. Presented data represent 10-min averages of original sensor measurements logged every 10 s. Two Mekong River waters were collected from an upstream (MK2) and a downstream (MK4) location of the Mekong-Tonle Sap confluence, while the mixture contained river water from MK2 and sewage from PP3 at the ratio of 9:1. In-stream  $pCO_2$  was measured using a membrane-enclosed sensor near the incubation bottles immersed in the surface water. (Color figure online)

## Discussion

Seasonality in *p*CO<sub>2</sub> and DOM composition in the Mekong–Tonle Sap

Higher levels of  $pCO_2$  observed in the Mekong reach upstream of the Tonle Sap confluence during the two monsoon surveys than in the dry season are consistent with the seasonal patterns reported for some Mekong sites upstream of Phnom Penh (Li et al. 2013) and in the Mekong Delta (Borges et al. 2018). Monsoonal increases in  $pCO_2$  were explained as a combined result of rainfall-enhanced flushing of soil CO<sub>2</sub> and OM and subsequent degradation of terrestrial OM during downstream transport (Li et al. 2013; Borges et al. 2018). Based on seasonal changes in the lignin-phenol composition, Ellis et al. (2012) suggested that OM derived from plants (angiosperms) might dominate fine particulate OM (FPOM) in the Lower Mekong River during the monsoon season. While most measurements varied little between the Mekong and Tonle Sap during the two monsoon surveys, indicating the prevailing effects of monsoonal floodwaters of the Mekong (Table 1, S1), the distinct differences in water quality at the most upstream Tonle Sap site (TS1) in August 2017 may indicate year-to-year variations in the effect of the Mekong floodwater intrusion on the Tonle Sap water quality. During the relatively dry years from 2015 to 2017, the reversed flows of the Tonle Sap decreased by  $\sim 9~{\rm km}^3$  compared to the long-term average (Mekong River Commission 2019).

The large divergences in  $pCO_2$  and  $\delta^{13}C-CO_2$ between the Tonle Sap and the Mekong reaches in January 2017 (Fig. 2) emphasize stronger dry-season impacts of the tributary carrying carbon components derived from the Lake Tonle Sap and downstream inputs of urban sewage than in the monsoon season. The dual isotope plots of  $\delta^{13}$ C and  $\Delta^{14}$ C of DOC and DIC (Fig. 3), combined with the values of  $\delta^{13}$ C-CO<sub>2</sub> (Table 1), provide additional evidence for the stronger dry-season tributary effects on DOM biodegradation and CO<sub>2</sub> production along the lower reach of the Tonle Sap and the downstream Mekong reaches. While the  $\Delta^{14}$ C-DIC values measured in the Mekong-Tonle Sap (-45.6%) to -62.7%; Fig. 3) were close to the reported values measured at MK2 during 2004 (-106%) to -63%; Martin et al. 2013), the dual isotopic signatures of DOC (Fig. 3) exhibited larger variations than the DOC values of  $\delta^{13}$ C (-26.2% to -27.2%) and  $\Delta^{14}$ C (-3\% to 52\%) reported by Martin et al. (2013). According to the year-long analysis focusing on the isotopic composition of FPOM at MK2,  $\Delta^{14}$ C-FPOM increased distinctively from the lowest value of -308% in the low-flow period up to 26‰ during the monsoon peak flow, unlike the rather modest seasonal changes in  $\Delta^{14}$ C-DOC (Martin et al. 2013).

The larger seasonal variations in  $\delta^{13}C$  and  $\Delta^{14}C$  observed in this study can be explained by the dominant dry-season influence of the Tonle Sap on the upward shift in  $\Delta^{14}C$ -DOC from MK2 to MK3 and the higher dry-season values of  $\delta^{13}C$ -DOC in the Mekong than during the monsoon season (Fig. 3). Previous studies ascribed the elevated carbon content in suspended sediment (Martin et al. 2013) and changes in other chemical indicators, such as lower yields of lignin normalized to carbon and increased N to C ratios (Ellis et al. 2012), to increased contributions of phytoplankton biomass to the dry-season



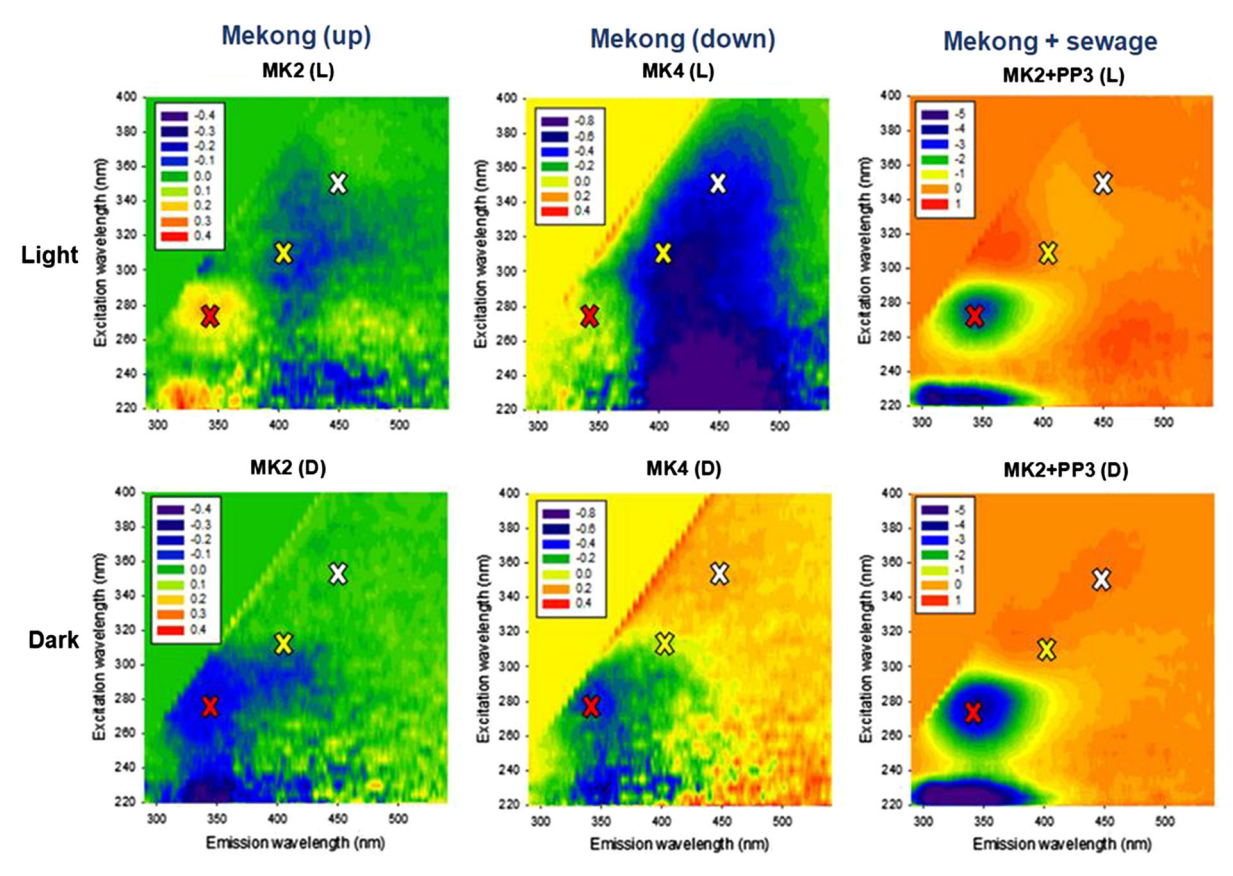


Fig. 5 Differential EEMs obtained by subtracting fluorescence intensities of the initial EEMs from those of the final EEMs measured before and after the in-situ incubation of the Mekong waters and sewage mixtures for 3 days. Positive and negative numbers indicate increases and decreases in fluorescence intensities during the incubation, respectively. Three major

fluorescent DOM components identified by PARAFAC modeling—C1 (ex/em: 350/450 nm), C2 (275/345 nm), C3 (310/405 nm)—are indicated by white, red, and yellow "X" symbols respectively. Refer to Fig. 4 for sample descriptions and Fig. S2 for the three PARAFAC components. (Color figure online)

POC. The value of  $\Delta^{14}$ C-DOC at MK2 in January 2017 was similar to the range of  $\Delta^{14}$ C -DIC measured in July 2014 (Fig. 3), which, along with the very low levels of  $pCO_2$  observed at MK1 and MK2 in January 2017 (Table 1), implies a dominant influence of phytoplankton on the Mekong carbon dynamics during the dry season. However, the distinct increase in  $\Delta^{14}$ C-DOC at MK3 toward the values found in the Tonle Sap (Fig. 3) suggests that the Tonle Sap inflow enriched in  $CO_2$  (particularly  $^{13}$  C in  $CO_2$ ) and labile DOM can drastically change the balance between autotrophy and heterotrophy along the downstream Mekong reaches during the dry season.

The low range of  $\Delta^{14}\text{C-DOC}$  (-145.1‰ to -94.4‰) observed at the two sewage drain sites (PP3 and PP4) is equivalent to an average age of 940 years BP and is similar to the reported range of  $\Delta^{14}\text{C}$ 

(-113.5% to -97.9%) measured for the DOC in effluents from a wastewater treatment plant (WWTP) in Korea (Jin et al. 2018), indicating a significant contribution of petroleum-based products such as detergents and pharmaceuticals (Griffith et al. 2009). The upward shift in  $\Delta^{14}$ C-DOC along the Tonle Sap in January 2017 (Fig. 3) may appear contradictory to the influence of  $^{14}$ C-depleted sewage OM. One potential explanation may be the preferential consumption of labile sewage-derived OM, leading to enrichment of  $^{14}$ C in the remaining organic pool.

Wastewater-fueled biodegradation during the dry season

The in situ incubation experiment results (Table 2; Figs. 3 and 4) illustrate that the effect of sewage



addition on the riverine CO<sub>2</sub> level can change not only longitudinally along the downstream reach but also temporally on a diel scale, as the balance between OM biodegradation and phytoplankton CO<sub>2</sub> uptake varies with light availability. For example, a large initial nocturnal increase in  $pCO_2$  in the sewage-supplemented river water was followed by a smaller daytime CO<sub>2</sub> uptake in the mixture treatment incubated under natural light conditions (Table 2). This result, combined with the preferential consumption of labile protein-like components of DOM shown on fluorescence EEMs (Fig. 5), indicates a sewage-induced stimulation of biodegradation of otherwise recalcitrant riverine DOM components during the dry season. When the untreated sewage from site PP3 was compared with a treated sewage effluent from a WWTP in Korea in a separate incubation experiment, the biodegradable DOC (BDOC) concentration was 31 times higher than that of the WWTP effluent, implying a very high lability of the DOM contained in the untreated sewage (Kim et al. 2019).

In the Mekong-only water from MK4, the initial nocturnal CO2 increase was smaller than that of the mixture samples, and the slightly larger nocturnal CO<sub>2</sub> production than the daytime uptake of CO<sub>2</sub> observed during the first day was reversed in the following two days (Table 2). However, this result cannot simply mean that the Tonle Sap inflow transformed the downstream Mekong reach into a CO2 sink under actual field conditions. As observed in the mixture samples (Table 2) and the separate laboratory incubation experiment with the sewage sample from PP3 (Kim et al. 2019), the rapid biodegradation of sewagederived OM may have tipped the balance toward CO<sub>2</sub> production outweighing consumption within a short period (< 1 d) during which unregulated river waters, such as those of the Mekong, can travel a long distance. The high-frequency in-stream measurements of pCO<sub>2</sub> at MK5 within a few kilometers away from MK4 showed some slight daytime decreases in  $pCO_2$ , but these downturns often lapsed into irregular concentration increases even during the day (Fig. 4), implying that the phytoplankton uptake of CO<sub>2</sub> may not fully offset sewage-fueled production of CO<sub>2</sub> in the affected downstream reach.

Distinct differences in differential EEMs between the Mekong-only treatments incubated under the two different light conditions indicated a potential synergistic effect of labile materials derived from phytoplankton on the biodegradation of DOM mixtures in the Mekong (Fig. 5). While simultaneous production and consumption of fluorescent DOM components have been observed in other studies of DOM biodegradation employing dark incubation (Guillemette and del Giorgio 2012; Jung et al. 2015; Begum et al. 2019), the consumption of protein-like fluorescence components and the production of humic-like fluorescence components were more commonly observed in these studies. Given the preferential consumption of algal DOM by bacterioplankton (Bianchi 2011; Bianchi et al. 2015; Guillemette et al. 2016), labile algal materials newly produced under light conditions might have been degraded faster than other DOM components, stimulating further bacterial consumption of humic-like DOM components. This proposition is consistent with the hypothesis that algal DOM primes the bacterial utilization of terrestrial DOM (Bianchi 2011; Bianchi et al. 2015) and the experimental demonstration of algal DOM facilitating the bacterial assimilation of terrestrial DOM (Guillemette et al. 2016). Therefore, the enhanced proteinlike fluorescence may reflect the production of new DOM components derived from the growing biomass of bacteria and/or phytoplankton. The sharp fluorescence decreases across the humic-like peaks (C1 and C3) in the MK4 samples incubated under natural light conditions (Fig. 5) suggest the contribution of both biodegradation and photodegradation to DOM transformations in the light. First, enhanced biodegradation might have depleted the pool of labile materials, triggering further processing of the bulk DOM pool and leading to the consumption of recalcitrant humic materials. Second, decreased fluorescence intensities of the humic-like peaks may also be associated with enhanced photodegradation at high daytime light intensities. Previous incubation experiments employing molecular-level analysis of photo-labile DOM components suggested that solar irradiation can remove refractory aromatic compounds including polyphenols and condensed aromatics derived from vascular plants during relatively short periods of incubation (Stubbins et al. 2010; Ward et al. 2017).

Increased DOC concentrations in the Mekong-only samples under both natural light and all-dark conditions imply that new DOC materials, either from newly produced phytoplankton biomass or transformed from POC, might have outpaced the biodegradation of the initial DOC pool. Although it would be



difficult to differentiate the primary source of CO<sub>2</sub> between the initial pool of DOC and the labile portion of POC, the initial spike of CO<sub>2</sub> production in the mixture samples provides a clear indication of high biodegradability of sewage-derived OM and its potential to accelerate the degradation of the recalcitrant original riverine OM that was indicated by a very small initial nocturnal CO<sub>2</sub> production in the MK2 sample (0.07 mg C  $L^{-1}$ ). Incubation experiments conducted with unfiltered river waters have reported considerable biodegradation rates of labile POC moieties in temperate rivers and estuaries (Etcheber et al. 2007; Jung et al. 2015) and tropical systems such as the Amazon (Ward et al. 2013, 2019). The high lability has been attributed to metabolically active particle-bound microbes that transform the labile fraction within suspended particles and dissolved constituents (Satinsky et al. 2017; Ward et al. 2019). As introduced earlier, Ellis et al. (2012) found in the Lower Mekong River that phytoplankton-derived materials constitute a greater proportion of FPOM during the dry season than during the monsoon period.

Implications for regional and global riverine carbon budgets

Although the tropics account for 56 and 61% of the global riverine fluxes of DOC and POC, respectively (Ludwig et al. 1996), OM transformations and CO<sub>2</sub> emissions in large tropical rivers remain poorly understood. Compared to other large river basins, only a small number of studies have estimated CO<sub>2</sub> emissions from the lower Mekong River and its tributaries (Alin et al. 2011; Li et al. 2013; Borges et al. 2018). To our knowledge, this study represents the first attempt to report direct pCO<sub>2</sub> measurements in the lower Mekong reach downstream of Phnom Penh. Alin et al. (2011) measured  $pCO_2$  along the Lower Mekong, but up to a location near site MK2. Li et al. (2013) and Borges et al. (2018) estimated CO<sub>2</sub> emissions from the entire Lower Mekong Basin and the Mekong Delta, respectively, but only based on calculated pCO<sub>2</sub> values using a carbon equilibrium model with measured alkalinity, pH, and water temperature as input data. Li et al. (2013) calculated  $pCO_2$  for 11 mainstem stations along the Lower Mekong during 1972-1998, which averaged 1090 μatm, falling in the range of pCO<sub>2</sub> measured by Alin et al. (2011) at locations near Vientiane and Phnom Penh (703–1257  $\mu$ atm). These measured or calculated values of  $pCO_2$  are relatively low compared with the global average (3100  $\mu$ atm) of the calculated values for 6708 stream and river locations worldwide (Raymond et al. 2013). By extrapolating the relatively low  $CO_2$  emission rate (195 mmol m<sup>-2</sup> d<sup>-1</sup>; 71 mol m<sup>-2</sup> yr<sup>-1</sup>) of the Lower Mekong for the entire Mekong Basin, Li et al. (2013) provided a modest estimate of the annual  $CO_2$  emission from the basin (71 mol m<sup>-2</sup> yr<sup>-1</sup>; 6.8 Tg  $CO_2$ –C yr<sup>-1</sup>).

Our observation of large seasonal and longitudinal variations in  $pCO_2$  (381–3119 µatm) along the Mekong around Phnom Penh raises the possibility of tributary-driven seasonal shifts in mainstem CO<sub>2</sub> emissions from the Lower Mekong Basin. Li et al. (2013) found some downstream increases in  $pCO_2$ along the Lower Mekong but did not consider the section downstream of the Tonle Sap confluence, thereby missing large downstream increases in CO<sub>2</sub> concentrations and fluxes during the dry season, as shown in this study (Table 1; Fig. 2). Using the  $pCO_2$ values measured in this study and the reported values of gas transfer velocity  $(k_{600})$  for the monsoon period (6.02 m d<sup>-1</sup>; Alin et al. 2011) and the dry season  $(2.01 \text{ m d}^{-1}; \text{Borges et al. } 2018)$ , the areal rate of  $CO_2$ emission from the Mekong mainstem is estimated to range from 171.5 to 363.5 mmol  $m^{-2} d^{-1}$  and from -4.2 to 231.2 mmol m<sup>-2</sup> d<sup>-1</sup> during the monsoon and dry season, respectively. While the overall average emission rate (258.6 mmol m<sup>-2</sup> d<sup>-1</sup>) is similar to the basin-wide average of 195 mmol m<sup>-2</sup> d<sup>-1</sup> estimated for the Lower Mekong by Li et al. (2013), the very large dry-season variations suggest that the sewageladen Tonle Sap inflow and presumably organic loads from other tributaries along the downstream reaches in Cambodia and Vietnam can shift the lower reaches of the Mekong from a weak sink or source to a significant source during the several consecutive dry months. Further research involving more frequent sampling at more sites is required to confirm and expand our exploratory findings that have limitations in terms of both spatial coverage and temporal resolution.

The unexpectedly high rates of dry-season  $CO_2$  emissions from the Tonle Sap carrying urban wastewater emphasize the need to assess wastewater effects on the emissions of  $CO_2$  and other greenhouse gases from urbanized river systems worldwide. As mentioned earlier, Regnier et al. (2013) provided a literature-based estimate of sewage contribution to



the global terrestrial C export to inland waters (0.1 Pg C yr<sup>-1</sup>). However, the global CO<sub>2</sub> emissions from wastewater and downstream rivers remain to be estimated. The findings of the elevated dry-season CO<sub>2</sub> emissions along the sewage-impacted Tonle Sap and Mekong reaches, combined with the very high lability of the DOM in untreated sewage as shown in the companion study (Kim et al. 2019), suggest that CO<sub>2</sub> emissions from large rivers receiving untreated domestic and industrial wastewater and agricultural runoffs across developing countries with poor wastewater infrastructure may exceed the levels found in the less impacted rivers to such a degree that can substantially increase the current estimates of global riverine CO2 emissions neglecting highly polluted rivers (e.g., Lauerwald et al. 2015).

## Conclusions

Despite the limited spatial coverage and temporal resolution of this study, the combination of seasonal comparison with high-frequency underway measurements of  $pCO_2$  and the dual isotope analysis of DOC provided the first field-based data documenting the pronounced dry-season influence of the Tonle Sap inflow carrying urban sewage on the OM degradation and CO<sub>2</sub> dynamics of the downstream Mekong reaches within the Phnom Penh metropolitan area. In contrast, the Mekong floods reversing the Tonle Sap during the monsoon season appear to homogenize the pCO<sub>2</sub> and DOM composition across the connected rivers. A noteworthy finding is that the influence of the Tonle Sap can switch the dry-season metabolic regime of the Mekong from autotrophic to heterotrophic dominance along a short stretch around the confluence. This finding has significant implications for the role of the Mekong reaches downstream of the Tonle Sap confluence as a source of CO<sub>2</sub> during several dry months, which in turn emphasizes the unexplored significance of the Tonle Sap Lake–River system as a source of OM and CO2 for the lower reaches of the Mekong. Light-enhanced DOM transformations in the sewage-impacted Tonle Sap and Mekong reaches imply the contributions of biodegradation and photodegradation, the relative importance of which remains to be investigated. Further research is also required to elucidate how the relative importance of the Tonle Sap Lake and downstream anthropogenic sources, such as urban sewage drains, changes as providers of labile DOM and CO<sub>2</sub> for the Tonle Sap and the connected downstream reaches of the Mekong throughout the year. Given the rising riverine organic pollution resulting from inadequate wastewater infrastructure across developing countries, the sewage-enhanced CO<sub>2</sub> emissions observed in the Mekong-Tonle Sap system may be common in many sewage-laden rivers worldwide. Therefore, more field-based studies in these understudied rivers may substantially alter the estimates of global riverine CO<sub>2</sub> emissions.

Acknowledgements We thank Sun-Hye Kim, Borami Park, Omme K. Nayna, Yewon Chun, Chhengngunn Aing, Zongta Sang, and many students at the Royal University of Phnom Penh for their assistance with sampling and sample analysis. We also gratefully acknowledge that Dr. Sanjeev Kumar at the Physical Research Laboratory helped us with the POC analysis and that Dr. Ishi Buffam and two anonymous reviewers provided us with helpful comments and suggestions.

**Funding** This work was supported by the Asia-Pacific Network for Global Change Research (CRRP2016-01MY-Park) and the National Research Foundation of Korea funded by the Korean Government (NRF-2017R1D1A1B06035179).

**Data availability** Data are available and can be requested from the corresponding author (jhp@ewha.ac.kr).

#### **Declarations**

**Conflict of interest** The authors declare that they have no conflicts of interest.

# References

Abril G, Nogueira E, Hetcheber H, Cabecadas G, Lemaire E, Brogueira MJ (2002) Behaviour of organic carbon in nine contrasting European estuaries. Estuar Coast Shelf Sci 54:241–262

Alin SR, Rasera MFFL, Salimon CI, Richey JE, Holtgrieve GW, Krusche AV, Snidvongs A (2011) Physical controls on carbon dioxide transfer velocity and flux in low-gradient river systems and implications for regional carbon budgets. J Geophys Res 116:G01009

Battin TJ, Luyssaert S, Kaplan LA, Aufdenkampe AK, Richter A, Tranvik LJ (2009) The boundless carbon cycle. Nature Geosci 2:598–600

Baum R, Luh J, Bartram J (2013) Sanitation: a global estimate of sewerage connections without treatment and the resulting impact on MDG progress. Environ Sci Technol 47:1994–2000



- Begum MS et al (2019) Synergistic effects of urban tributary mixing on dissolved organic matter biodegradation in an impounded river system. Sci Total Environ 676:105–119
- Begum MS et al (2021) Localized pollution impacts on greenhouse gas dynamics in three anthropogenically modified Asian river systems. J Geophys Res Biogeosci 126:e2020JG006124. https://doi.org/10.1029/ 2020JG006124
- Bengtsson MM, Attermeyer K, Catalán N (2018) Interactive effects on organic matter processing from soils to the ocean: are priming effects relevant in aquatic ecosystems? Hydrobiologia 822:1–17. doi:https://doi.org/10.1007/s10750-018-3672-2
- Bianchi TS (2011) The role of terrestrially derived organic carbon in the coastal ocean: a changing paradigm and the priming effect. Proc Natl Acad Sci USA 108:19473–19481. doi:https://doi.org/10.1073/pnas. 1017982108
- Bianchi TS, Thornton DC, Yvon-Lewis SA, King GM, Eglinton TI, Shields MR, Ward ND, Curtis J (2015) Positive priming of terrestrially derived dissolved organic matter in a freshwater microcosm system. Geophys Res Lett 42:5460–5467
- Borges AV, Abril G, Bouillon S (2018) Carbon dynamics and CO2 and CH4 outgassing in the Mekong Delta. Biogeosciences 15:1093–1114
- Campbell IC, Say S, Beardall J (2009) Tonle Sap Lake, the heart of the Lower Mekong. In: Campbell IC (ed) The Mekong—biophysical environment of an International River Basin. Elsevier, New York, pp 251–272
- Cole JJ, Prairie YT, Caraco NF, McDowell WH, Tranvik LJ, Striegl RG, Duarte CM, Kortelainen P, Downing JA, Middelburg JJ, Melack J (2007) Plumbing the global carbon cycle: Integrating inland waters into the terrestrial carbon budget. Ecosystems 10:171–184
- Crawford JT, Loken LC, Stanley EH, Stets EG, Dornblaser MM, Striegl RG (2016) Basin scale controls on CO<sub>2</sub> and CH<sub>4</sub> emissions from the Upper Mississippi River. Geophys Res Lett 43:1973–1979. doi:https://doi.org/10.1002/2015GL067599
- Ellis EE, Keil RG, Ingalls AE, Richey JE, Alin SR (2012) Seasonal variability in the sources of particulate organic matter of the Mekong River as discerned by elemental and lignin analyses. J Geophys Res 117:G01038. doi:https:// doi.org/10.1029/2011JG001816
- Etcheber H, Taillez A, Aril G, Garnier J, Servais P, Moatar F, Commarieu M-V (2007) Particulate organic carbon in the estuarine turbidity maxima of the Gironde, Loire and Seine estuaries: origin and lability. Hydrobiologia 588:245–259
- Fellman JB, Hood E, Spencer RGM (2010) Fluorescence spectroscopy opens new windows into dissolved organic matter dynamics in freshwater ecosystems: a review. Limnol Oceanogr 55:2452–2462. https://doi.org/10.4319/lo.2010.55.6.2452
- Frankignoulle M, Abril G, Borges A, Bourge I, Canon C, Delille B, Libert E, Théate J-M (1998) Carbon dioxide emission from European estuaries. Science 282:434–436
- Global Green Growth Institute (GGGI) (2019) Phnom Penh Sustainable City Plan 2018–2030. https://gggi.org/site/ assets/uploads/2019/06/SUBSTAINABLE-CITY-REPORT\_EN\_FA3.pdf (accessed on February 19, 2021)

- Griffith DR, Raymond PA (2011) Multiple-source heterotrophy fueled by aged organic carbon in an urbanized estuary. Marine Chem 124:14–22
- Griffith DR, Barnes RT, Raymond PA (2009) Inputs of fossil carbon from wastewater treatment plants to US rivers and oceans. Environ Sci Technol 43:5647–5651
- Guillemette F, del Giorgio PA (2012) Simultaneous consumption and production of fluorescent dissolved organic matter by lake bacterioplankton. Environ Microbiol 14:1432–1443
- Guillemette F, McCallister SL, del Giorgio PA (2016) Selective consumption and metabolic allocation of terrestrial and algal carbon determine allochthony in lake bacteria. ISME J 10:1373–1382
- Hosen JD, McDonough OT, Febria CM, Palmer MA (2014) Dissolved organic matter quality and bioavailability changes across an urbanization gradient in headwater streams. Environ Sci Technol 48:7817–7824
- Hudson F (2004) Sample preparation and calculations for dissolved gas analysis in water samples using GC headspace equilibration technique, RSKSOP-175, Revision No, 2. U.S. Environmental Protection Agency, USA
- Jin H, Yoon TK, Begum MS, Lee E-J, Oh N-H, Kang N, Park J-H (2018) Longitudinal discontinuities in riverine greenhouse gas dynamics generated by dams and urban wastewater. Biogeosciences 15:6349–6369. https://doi. org/10.5194/bg-15-6349-2018
- Jung B-J, Jeanneau L, Alewell C, Kim B, Park J-H (2015) Downstream alteration of the composition and biodegradability of particulate organic carbon in a mountainous, mixed land-use watershed. Biogeochemistry 122:79–99. https://doi.org/10.1007/s10533-014-0032-9
- Kempe S (1984) Sinks of the anthropogenically enhanced carbon-cycle in surface fresh waters. J Geophys Res 89:4657–4676. doi:https://doi.org/10.1029/JD089iD03p04657
- Kim D, Begum M, Choi J, Jin H, Chea E, Park J-H (2019) Comparing effects of untreated and treated wastewater on riverine greenhouse gas emissions. APN Sci Bull 9:88–94. doi:https://doi.org/10.30852/sb.2019.872
- Lauerwald R, Laruelle GG, Hartmann J, Ciais P, Regnier PAG (2015) Spatial patterns in CO<sub>2</sub> evasion from the global river network. Global Biogeochem Cy 29:534–554. doi:https://doi.org/10.1002/2014GB004941
- Li S, Lu XX, Bush RT (2013) CO<sub>2</sub> partial pressure and CO<sub>2</sub> emission in the Lower Mekong River. J Hydrol 504:40–56
- Ludwig W, Probst J-L, Kempe S (1996) Predicting the oceanic input of organic carbon by continental erosion. Global Biogeochem Cy 10:23–41. doi:https://doi.org/10.1029/ 95GB02925
- Martin EE, Ingalls AE, Richey JE, Keil RG, Santos GM, Truxal LT, Alin SR, Druffel ERM (2013) Age of riverine carbon suggests rapid export of terrestrial primary production in tropics. Geophys Res Lett 40:5687–5691. https://doi.org/10.1002/2013GL057450
- McKnight DM, Boyer EW, Westerhoff PK, Doran PT, Kulbe T, Anderson DT (2001) Spectroflourometric characterization of dissolved organic matter for indication of precursor organic material and aromaticity. Limnol Oceanogr 46:38–48. https://doi.org/10.4319/lo.2001.46.1.0038



- Mekong River Commission (2019) State of the Basin Report 2018, The Mekong River Commission, Vientiane, Lao PDR
- Park J-H, Nayna OK, Begum MS, Chea E, Hartmann J, Keil RG, Kumar S, Lu X, Ran L, Richey JE, Sarma VVSS, Tareq SM, Xuan DT, Yu R (2018) Reviews and syntheses: Anthropogenic perturbations to carbon fluxes in Asian river systems—concepts, emerging trends, and research challenges. Biogeosciences 15:3049–3069. https://doi.org/ 10.5194/bg-15-3049-2018
- Räsänen TA, Varis O, Scherer L, Kummu M (2016) Greenhouse gas emissions of hydropower in the Mekong River Basin. Environ Res Lett 13:034030
- Raymond PA, Bauer JE (2001) Use of <sup>14</sup> C and <sup>13</sup> C natural abundances for evaluating riverine, estuarine, and coastal DOC and POC sources and cycling: a review and synthesis. Org Geochem 32:469–485. doi:https://doi.org/10.1016/S0146-6380(00)00190-X
- Raymond PA, Hartmann J, Lauerwald R, Sobek S, McDonald, Hoover M, Butman D, Striegl R, Mayorga E, Humborg C, Kortelainen P, Dürr H, Meybeck M, Ciais P, Guth P (2013) Global carbon dioxide emissions from inland waters. Nature 503:355–359
- Regnier P, Friedlingstein P, Ciais P et al (2013) Anthropogenic perturbation of carbon fluxes from land to ocean. Nature Geosci 6:597–607
- Sabo JL, Ruhi A, Holtgrieve GW, Elliott V, Arias ME, Ngor PB, Räsänen TA, So N (2017) Designing river flows to improve food security futures in the Lower Mekong Basin. Science 358:eaao1053. DOI:https://doi.org/10.1126/science.aao1053
- Satinsky BM, Smith CB, Sharma S, Ward ND, Krusche AV, Richey JE et al (2017) Patterns of bacterial and archaeal gene expression through the lower Amazon River. Front Mater Sci 4:253. doi:https://doi.org/10.3389/fmars.2017. 00253
- Stedmon CA, Bro R (2008) Characterizing dissolved organic matter fluorescence with parallel factor analysis: a tutorial. Limnol Oceanogr Methods 6:572–579. https://doi.org/10.4319/lom.2008.6.572
- Stubbins A, Spencer RGM, Chen HM, Hatcher PG, Mopper K, Hernes PJ, Mwamba VL, Mangangu AM, Wabakanghanzi JN, Six J (2010) Illuminated darkness: Molecular

- signatures of Congo River dissolved organic matter and its photochemical alteration as revealed by ultrahigh precision mass spectrometry. Limnol Oceanogr 55(4):1467–1477
- Stubbins A, Lapierre J-F, Berggren M, Prairie YT, Dittmar T, del Giorgio PA (2014) Environ Sci Technol 48:10598–10606. doi:https://doi.org/10.1021/es502086e
- Ward CP, Nalven SG, Crump BC, Kling GW, Cory RM (2017)
  Photochemical alteration of organic carbon-draining permafrost soils shifts microbial metabolic pathways and stimulates respiration. Nature Comm 8:772
- Ward ND, Keil RG, Medeiros PM, Brito DC, Cunha AC, Dittmar T et al (2013) Degradation of terrestrially derived macromolecules in Amazon River. Nat Geosci 6:530–533. doi:https://doi.org/10.1038/ngeo1817
- Ward ND, Sawakuchi HO, Richey JE, Keil RG, Bianchi TS (2019) Enhanced aquatic respiration associated with mixing of clearwater tributary and turbid Amazon river waters. Front Earth Sci 7:101. doi:https://doi.org/10.3389/feart. 2019.00101
- Weishaar JL, Aiken GR, Bergamaschi BA, Fram MS, Fujii R, Mopper K (2003) Evaluation of specific ultraviolet absorbance as an indicator of the chemical composition and reactivity of dissolved organic carbon. Environ Sci Technol 37:4702–4708. https://doi.org/10.1021/es030360x
- Yoon TK, Jin H, Oh N-H, Park J-H (2016) Technical note: Assessing gas equilibration systems for continuous pCO<sub>2</sub> measurements in inland waters. Biogeosciences 13:3915–3930. https://doi.org/10.5194/bg-13-3915-2016
- Yoon TK, Jin H, Begum MS, Kang N, Park JH (2017) CO<sub>2</sub> outgassing from an urbanized river system fueled by wastewater treatment plant effluents. Environ Sci Technol 51:10459–10467. https://doi.org/10.1021/acs.est.7b02344
- Zsolnay A, Baigar E, Jimenez M, Steinweg B, Saccomandi F (1999) Differentiating with fluorescence spectroscopy, the sources of dissolved organic matter in soils were subjected to drying. Chemosphere 38:45–50. https://doi.org/10.1016/S0045-6535(98)00166-0

**Publisher's Note** Springer Nature remains neutral with regard to jurisdictional claims in published maps and institutional affiliations.

